Presentation Prepared for the Premixed-Prevaporized
Combustor Technology (PPCT) Forum
NASA Lewis Research Center, Jan 9-10, 1978

Turbulence Characteristics of Compressor Discharge Flows

Howard P. Grant, P&WA CPD E. Hartford

Turbulence measurements were conducted in a large gas turbine engine (JT9D) at the entrance to the diffuser duct, joining the compressor discharge to the combustor inlet. Hot film probe and hot wire probe measurements were obtained at temperatures from 450K (350F) (idle) to 608K (635°F) (rich approach).

The work was conducted at P&WA in East Hartford in late 1976 under NASA LeRC Contract NAS3-19447 as part of the ECCP - Experimental Clean Combustor Program. The detailed results are presented in report No. NASA CR-135277.

At I.D. (25 percent span) and mid-span locations, the turbulence intensity increased slightly from 6 ±1 percent at idle condition to 7±1 percent at rich approach. AT O.D. (75 percent span) the turbulent intensity increased more rapidly, from 7.5± 0.5 percent at idle to 15±0.5 percent at rich approach. The spectra showed turbulent energy distributed uniformly over a 0.1 to 5 KHz bandwidth (down 3 db) at all operating conditions, corresponding to random turbulence with velocity wave lengths of 2 cm to 1 meter travelling at the mean velocity of 100 m/sec. Above 5 KHz the turbulent energy decreased at a rate proportional to $f^{-0.25\pm0.1}$ in all cases, with roll-off frequency not a strong function of engine operating point.

The turbulence near the diffuser O.D. is large enough in amplitude and scale to affect the flow to the front end sections of the burner. The origin of this high turbulence level requires further information on the turbulence development along the diffuser.

Velocity fluctuations at blade-passing frequency (about 10KHz) were identifiable at all spanwise positions, but the amplitude and scale were not large enough to affect the combustor flow.

Measurements at higher engine power levels are of course needed to determine whether shifts in amplitude or scale of turbulence occur. Laser Doppler anemometer optical instrumentation should be considered for these higher power studies, since the 608K temperature is the upper limit for state-of-the-art hot wire or hot film probes in the engine environment. Hot wires are capable of operation at stream temperatures to at least 800K (1000°F), but only in extremely clean air streams free of foreign matter. In fact all the hot wires tried in the engine failed in a matter of minutes. The hot film probes are orders of magnitude more durable and all but one survived the entire 3 day engine test. Films, however, can not be used at stream temperatures above 615K (650°F) because thermally induced stresses in the sensor head exceed the strength of the quartz insulating material.

Measurements of this kind in the compressor exit environment are difficult, requiring meticulous attention to preliminary calibration, data acquisition procedure, and automated data reduction procedures. The sensors are continuously threatened with destruction by foreign object damage in the engine, so operating time on the engine test stand must be used efficiently, and provision for quick change of probes must be included in the installation scheme used.

The engine, test cell, combustor cross section, and turbulence probe locations are shown in Figs 1 through 5. The probes used are described in Table 1 and Figs 6,7 and 8.

Note particularly in Fig 7 that each probe was equipped with a mounting boss with depth preset, and alignment with engine axis predetermined. Replacement probes could be inserted in a few minutes.

A series of special calibrations was carried out with each probe in the laboratory. The first calibration was sensor resistance vs. temperature (Fig 9) to determine the maximum safe operating resistance for each sensor. Next each sensor was inserted in a conventional commercial anemometer bridge circuit of the constant resistance type, in which a feedback circuit automatically varies the bridge voltage (i.e. sensor heating current) to mantain the sensor at the selected constant resistance. The bridge voltage was then measured as a function of gas temperature at zero flow (Fig 10) and as a function of gas velocity at room temperature (Figs 11 and 12). This provides all the information needed for calculation of d.c. velocity sensitivity at any combination of gas velocity and gas temperature. The equations are presented in the referenced report. The frequency response of each probe was then determined by comparison with a 6μ platinum wire probe (known to have flat response beyond 20 KHz) in a turbulent jet, and a transfer function (frequency response correction function) constructed for each probe. An example is shown in Fig 13. The transfer function was found not to be a strong function of Reynolds number.

The data acquisition system (magnetic tape) and playback system is shown in Fig 14. The key to success in playback is the use of the spectrum analyzer and the mini-computer programmed with the calibration equations that permitted calculation of the turbulence energy content of each of 399 frequency intervals 50 Hz wide, covering the 0.1 to 20 KHz frequency range. From this information the minicomputer was able to output spectrum plots, turbulence intensity, integral scale, and microscale, using the Hinze turbulence relations.

The results are presented numerically in tables II, III, IV, V, and VI and graphically in Figures 15 through 26.

Figure 15 is a plot of all validated turbulence data, showing the trends already discussed.

Fig. 16 is a typical spectrum plot, showing the classical random turbulence spectrum, except that it is punctuated with spikes at blade passing frequency (about 10 KHz) and at twice blade passing frequency. The energy in these spikes is small. The weak peak at about 900Hz at 75% span (Figs 18,19) is unexplained, by the way. Rotor frequency was below 100 Hz.

Note again that the turbulent scale is quite large. 5 KHz component corresponds to an axial scale of about 2 cm. Most of the random energy is contained in velocity wave lengths between 1.0 meter and 2 cm.

Finally it is interesting to note that the large turbulence level at O.D. may improve the performance of the diffuser by retarding separation.

The program illustrates well the capability of sophisticated anemometer instrumentatio to produce valuable data under extremely difficult conditions, when sufficient care an feeding is supplied.

TABLE I

PROBE TYPES AND LOCATIONS

Test No. 1

*Probe No.	Type	Angular Location	Spanwise Location (Percent)
1	370μ diameter Stainless Steel Wire Probes	323° 05′	25, 50, 75
2	TSI 949K Hot Film Probes	358° 22′	25, 50, 75
3	TSI 949K Hot Film Probes	17° 52′	25, 50, 75
4	TSI 949K Hot Film Probes	143° 04′	25, 50, 75
5	370μ diameter Stainless Steel Wire Probes	178° 18′	25, 50, 75
6	12μ Pt-Ir Wire Probes	217° 25′	25, 50, 75

Test No. 2

*Probe No.	Type	Angular Location	Spanwise Location (Percent)
1	370μ diameter Stainless Steel Wire Probes	323° 05′	25, 50, 75
2	370μ diameter Stainless Steel Wire Probes	358° 22′	25, 50, 75
3	370μ diameter Stainless Steel Wire Probes	17° 52′	25, 50, 75
4			
5	370μ diameter Stainless Steel Wire Probes	178° 18′	25, 50, 75
6	12μ Pt - Ir Wire Probes	217° 25′	25, 50, 75

Test No. 2

*Probe No.	Type	Angular Location	Spanwise Location (Percent)
1	TSI 949K Hot Film Probe	323° 05′	25, 50, 75
2	TSI 949K Hot Film Probe	358° 22′	25, 50, 75
3	TSI 949K Hot Film Probe	17° 52′	25, 50, 75
4	TSI 949K Hot Film Probe	143° 04′	25, 50, 75
5	TSI 949K Hot Film Probe	178° 18′	25, 50, 75
6	TSI 949K Hot Film Probe	217° 25′	25, 50, 75

*See Figure 5 for Probe Location

TABLE II

DEPENDENCE OF TURBULENT INTENSITY ON ENGINE OPERATION, TEST 1

Test Point	Designation	Probe 1 S.S. Wire 323° 5′ 50% Span		Probe 2 Hot Film 358° 22′ 50% Span		Probe 3 Hot Film 17° 52′ 25% Span		Probe 4 Hot Film 143° 04′ 75% Span		Probe 5 S.S. Wire 178° 18′ 50% Span		Probe 6 Pt.-Ir. Wire 217° 25′ 50% Span	
		T_4 K	$Tu/\bar{u}$ %	T_4 K	$Tu/\bar{u}$ %	T_4 K	$Tu/\bar{u}$ %	T_4 K	$Tu/\bar{u}$ %	T_4 K	$Tu/\bar{u}$ %	T_4 K	$Tu/\bar{u}$ %
1	Idle	Failed		450	7.0	454	4.76	Erratic		Erratic		Failed	
2	Flight Idle	Failed		516	8.16	Erratic		Erratic		Erratic		Failed	
3	Approach	Failed		591	7.64	597	6.65	Erratic		Erratic		Failed	
4	Idle	Failed		456	6.59	464	4.78	Erratic		Failed		Failed	
5	Rich Approach	Failed		608	7.96	616	5.42	Erratic		Failed		Failed	
6	Idle	Failed		455	5.22	455	4.81	Erratic		Failed		Failed	

TABLE III

DEPENDENCE OF TURBULENT INTENSITY ON ENGINE OPERATION, TEST 2

Test Point	Designation	Probe 1 S.S. Wire 323° 05′ 25% Span		Probe 2 S.S. Wire 358° 22′ 75% Span		Probe 3 S.S. Wire 17° 52′ 50% Span		Probe 4 None Installed		Probe 5 S.S. Wire 178° 18′ 50% Span		Probe 6 Pt-Ir Wire 217° 25′ 25% Span	
		T_4 K	$Tu/\bar{u}$ %	T_4 K	$Tu/\bar{u}$ %	T_4 K	$Tu/\bar{u}$ %	T_4 K	$Tu/\bar{u}$ %	T_4 K	$Tu/\bar{u}$ %	T_4 K	$Tu/\bar{u}$ %
1	Climb	Failed		Failed		Failed		–	–	Erratic		Failed	

TABLE IV

DEPENDENCE OF TURBULENT INTENSITY ON ENGINE OPERATION, TEST 3

Test Point	Designation	Probe 1 Hot Film 323° 05′ 25% Span		Probe 2 Hot Film 358° 22′ 75% Span		Probe 3 Hot Film 17° 52′ 50% Span		Probe 4 Hot Film 143° 4′ 75% Span		Probe 5 Hot Film 178° 18′ 50% Span		Probe 6 Hot Film 217° 25′ 25% Span	
		T_4 K	$Tu/\bar{u}$ %	T_4 K	$Tu/\bar{u}$ %	T_4 K	$Tu/\bar{u}$ %	T_4 K	$Tu/\bar{u}$ %	T_4 K	$Tu/\bar{u}$ %	T_4 K	$Tu/\bar{u}$ %
1	Idle	461	6.83	452	7.09	Erratic		450	7.93	Erratic		459	5.87
2	Flight Idle	536	7.70	525	10.56	Erratic		520	11.03	Erratic		519	6.14
3	Approach	611	7.09	602	16.17	Erratic		597	14.17	Erratic		602	5.68
4	Idle	461	6.88	450	7.05	Erratic		447	8.08	Erratic		452	6.18

TABLE V

ENGINE TEST CONDITIONS

	Test Pt.	Designation	T_{T4}* K	P_{T4}* 10^5 N/m^2	Average Velocity Calculated From P_{T4}/T_{T4} m/sec	F/A	N_2 RPM	Fn N
Test 1	1	Idle	450	3.71	109.3	0.0096	4941	14052
	2	Flight Idle	520	6.02	112.2	0.0106	5765	31471
	3	Approach	590	9.17	122.8	0.0140	6376	61759
	4	Idle	452	3.76	108.9	0.0095	4983	14470
	5	Rich Approach	609	9.91	128.1	0.0148	6499	70366
	6	Idle	446	3.63	107.1	0.0095	4913	13549
Test 2	1	Climb	732	18.2	139.3	0.0227	7206	169030
Test 3	1	Idle	454	3.88	110.1	0.0102	4830	16436
	2	Flight Idle	520	6.16	119.2	0.0118	5557	35177
	3	Approach	599	9.77	125.7	0.0152	6203	72284
	4	Idle	449	3.80	122.1	0.0103	4801	16018

*Measured

TABLE VI

TURBULENCE CHARACTERISTICS OF COMPRESSOR DISCHARGE FLOWS

Hot Film Probe Number	Hot Film Probe Percent Span	Hot Film Probe Angular Location	Tu (meters/sec)	Turbulent Intensity $Tu/\bar{u}$	Λ (Macro-scale In Meters)	λ (Micro-scale In Meters)
2	50	358° 22′	6.782	0.06998	0.0079	0.0051
			8.556	0.08160	0.0116	0.0097
			8.620	0.07644	0.0083	0.0104
			6.471	0.06593	0.0094	0.0078
			9.145	0.07958	0.0124	0.0093
			5.103	0.05216	0.0169	0.0079
3	25	17° 52′	4.645	0.04762	0.0153	0.0094
			7.560	0.06650	0.0109	0.0076
			4.723	0.04782	0.0111	0.0082
			6.273	0.05416	0.0107	0.0090
			4.710	0.04814	0.0121	0.0089
1	25	323° 05′	6.725	0.06831	0.0212	0.0087
			8.209	0.07695	0.0099	0.0089
			8.163	0.07085	0.0086	0.0076
			6.774	0.06880	0.0181	0.0077
2	75	358° 22′	6.890	0.07086	0.0082	0.0079
			11.166	0.10557	0.0063	0.0085
			18.482	0.16169	0.0100	0.0058
			6.834	0.07050	0.0161	0.0071
4	75	143° 04′	7.683	0.07927	0.0323	0.0064
			11.561	0.11026	0.0162	0.0064
			16.104	0.14165	0.0104	0.0090
			7.807	0.08080	0.0333	0.0086
6	25	217° 25′	5.747	0.05873	0.0104	0.0081
			6.453	0.06136	0.0095	0.0083
			6.489	0.05677	0.0088	0.0077
			6.007	0.06178	0.0290	0.0072

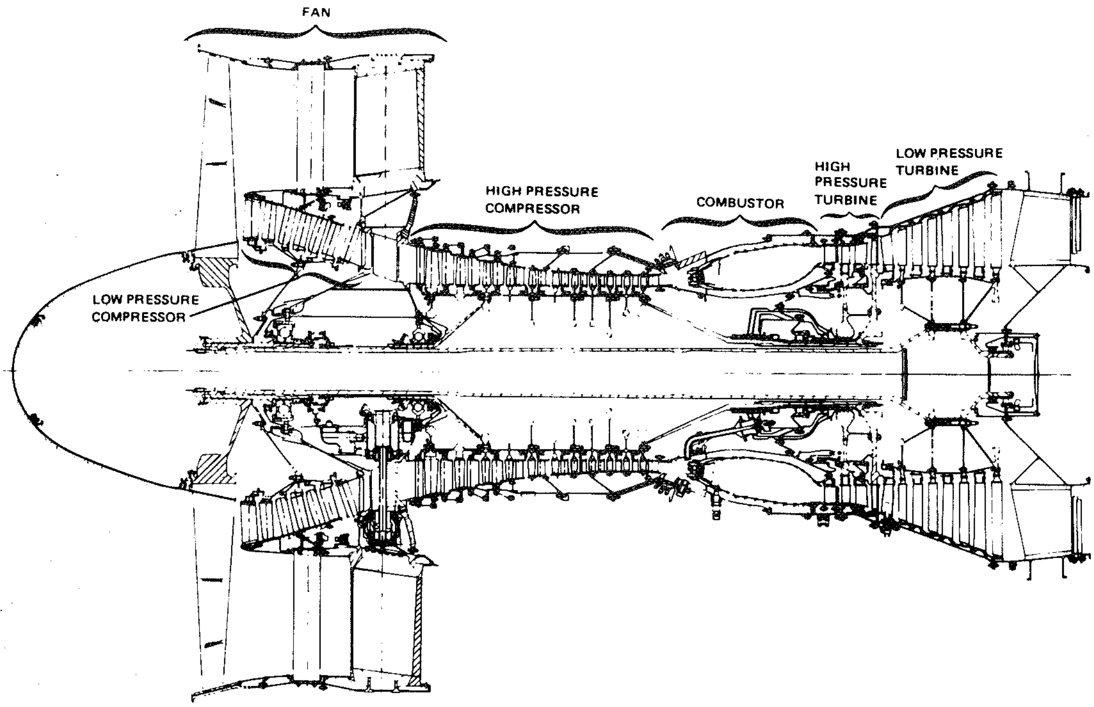

Figure 1 Cross Sectional Schematic of the JT9D-7A Reference Engine

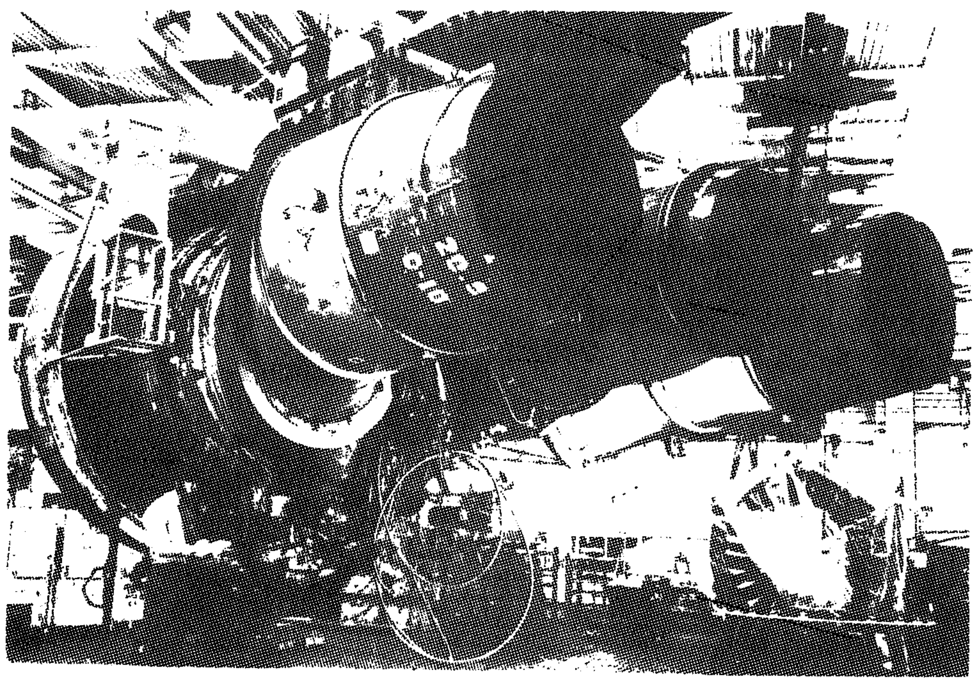

Figure 2 Experimental Engine, X-686, With Bifurcated Ducts Installed (X-43208)

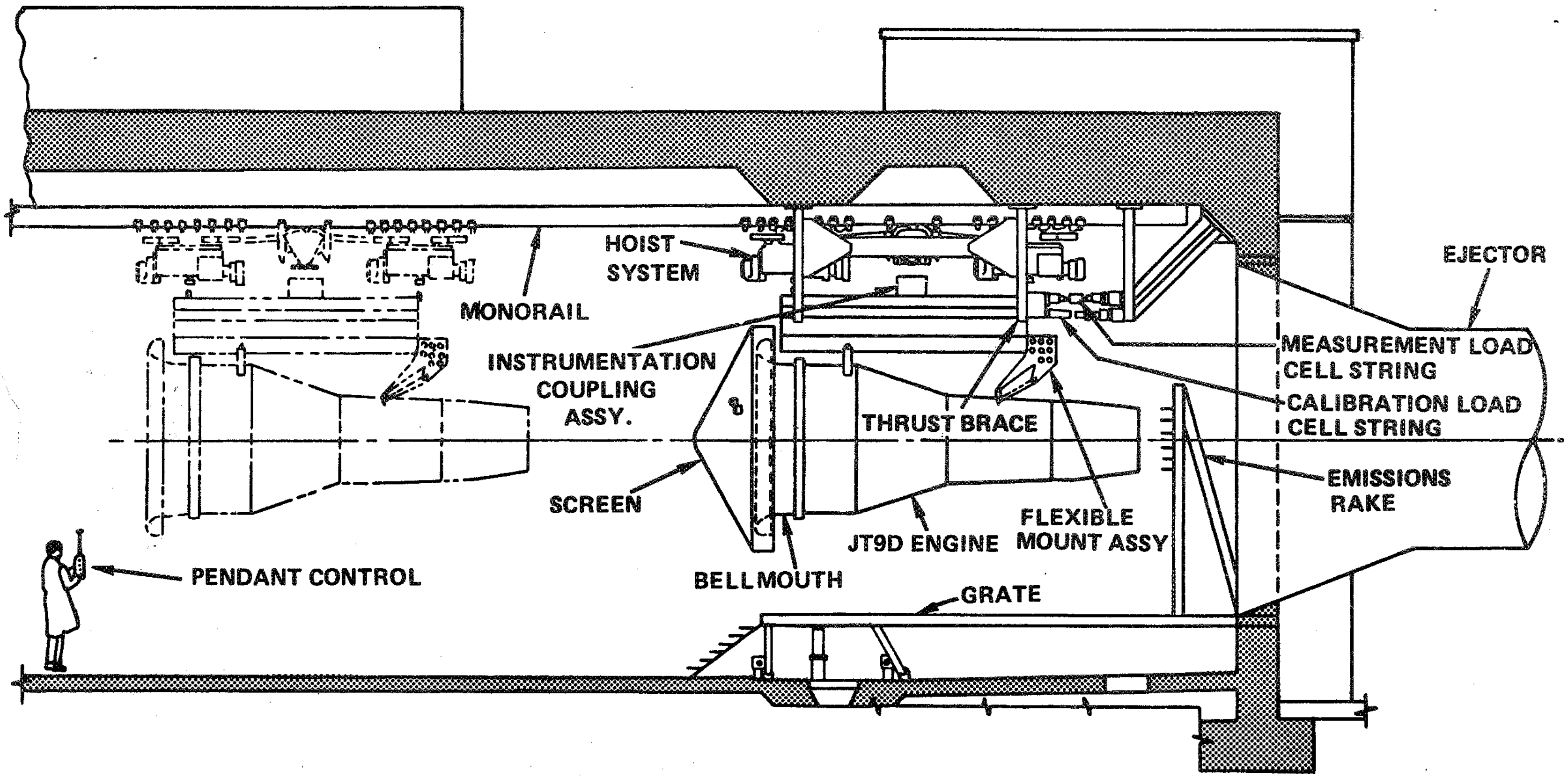

Figure 3 P-6 Test Cell Layout

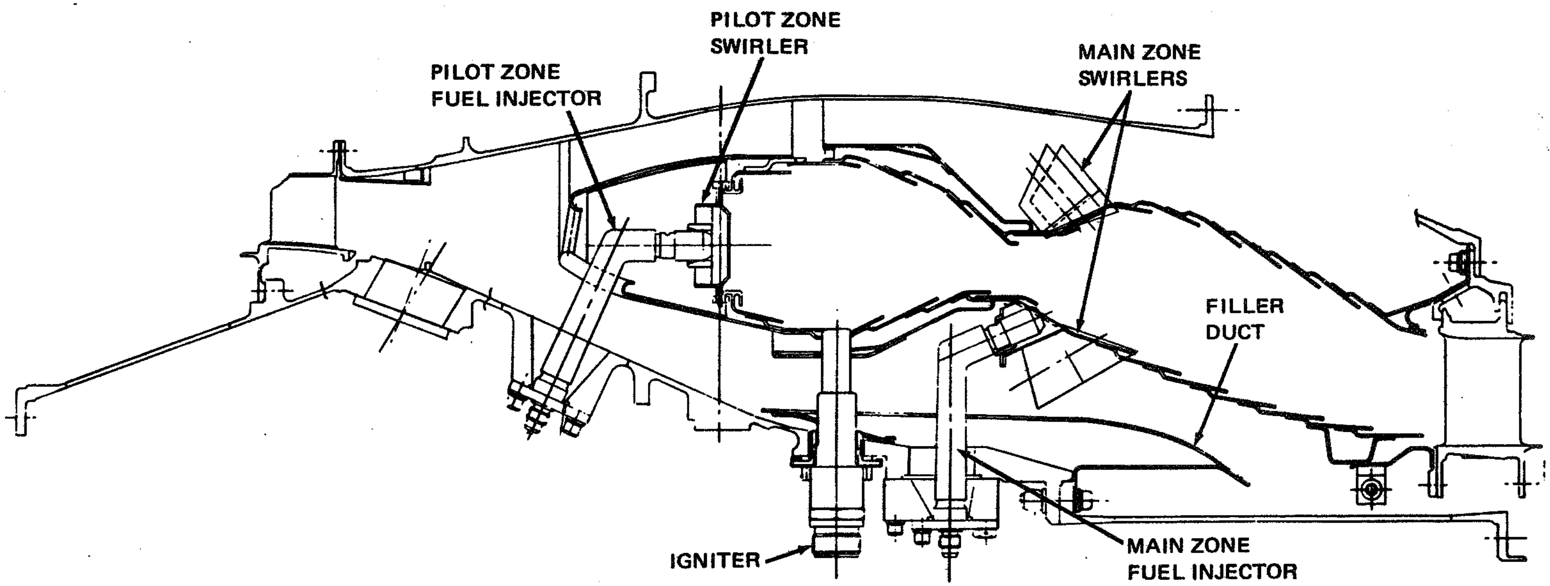

Figure 4 Cross Section of Experimental Clean Combustor Program Phase III Vorbix Combustor

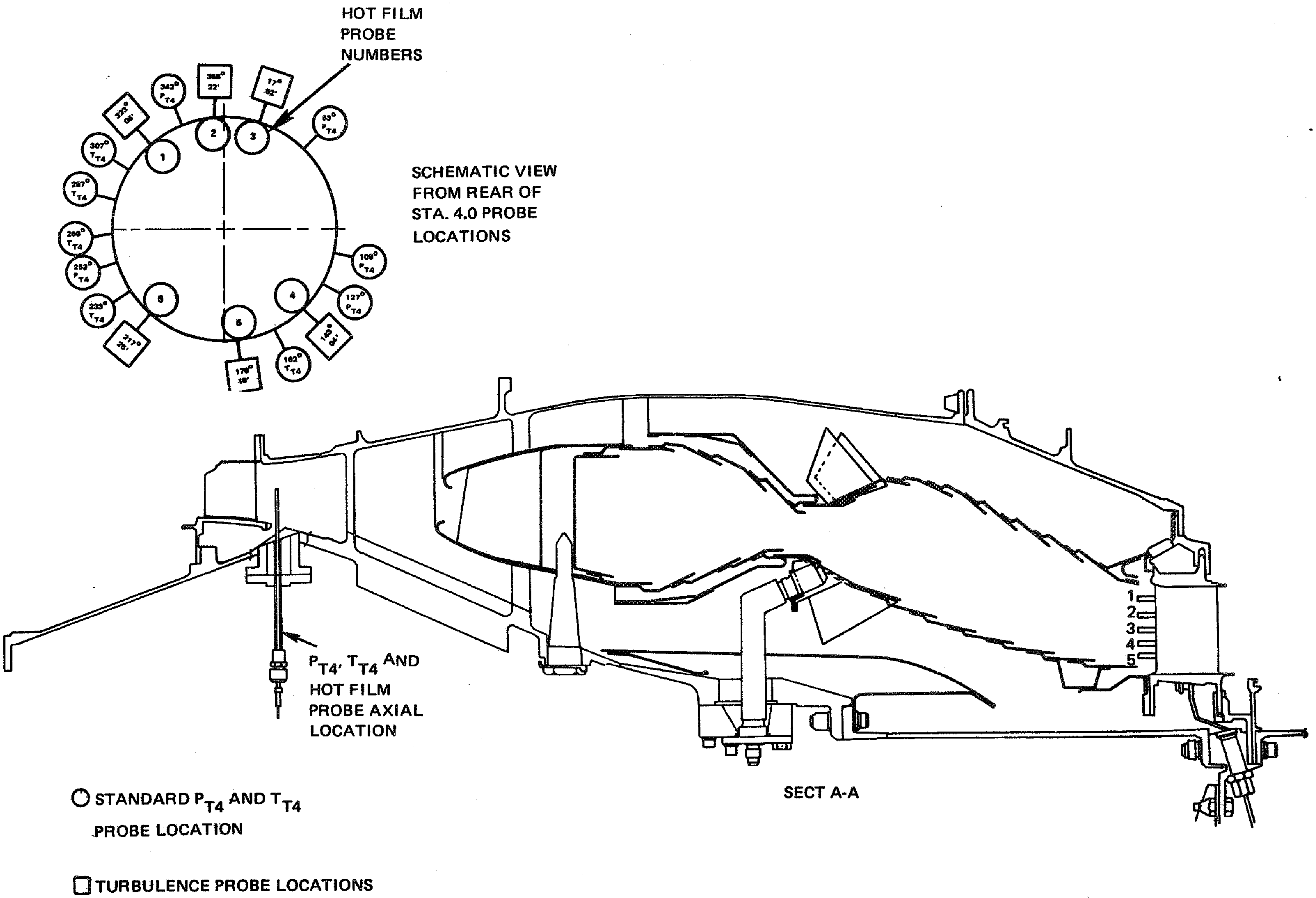

Figure 5 Location of Turbulence Probes

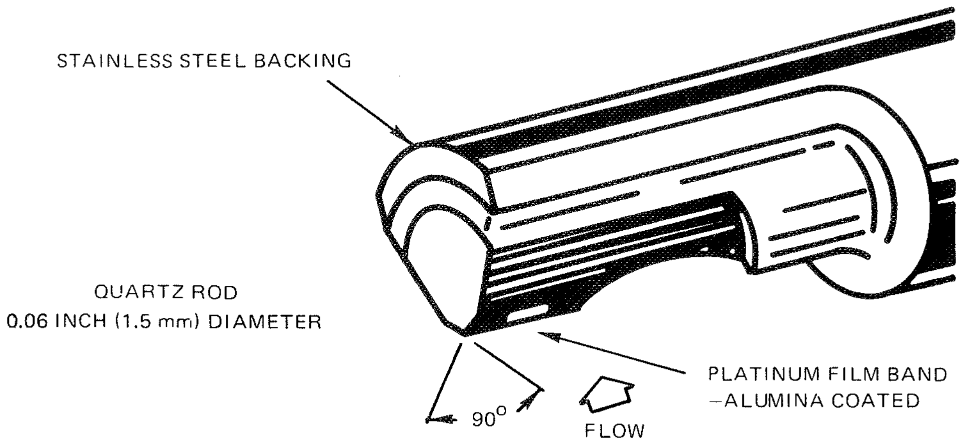

SENSING SIZE: TWO WEDGE SURFACES EACH 0.005 INCH (0.12 mm) WIDE BY 0.04 INCH (1.0 mm) LONG

(a)

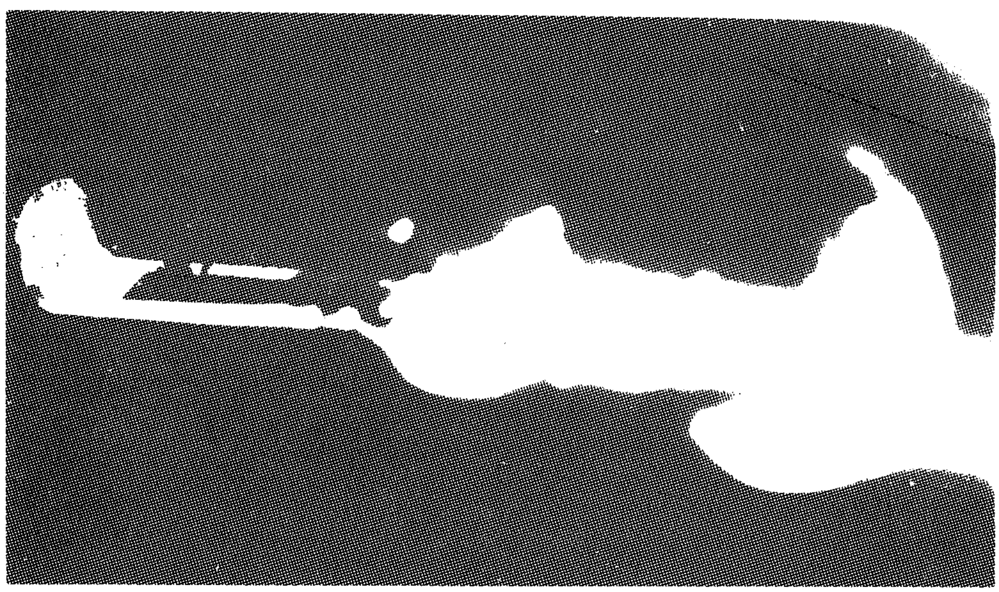

(b)

Figure 6 Wedge Type Probe (77-444-9004)

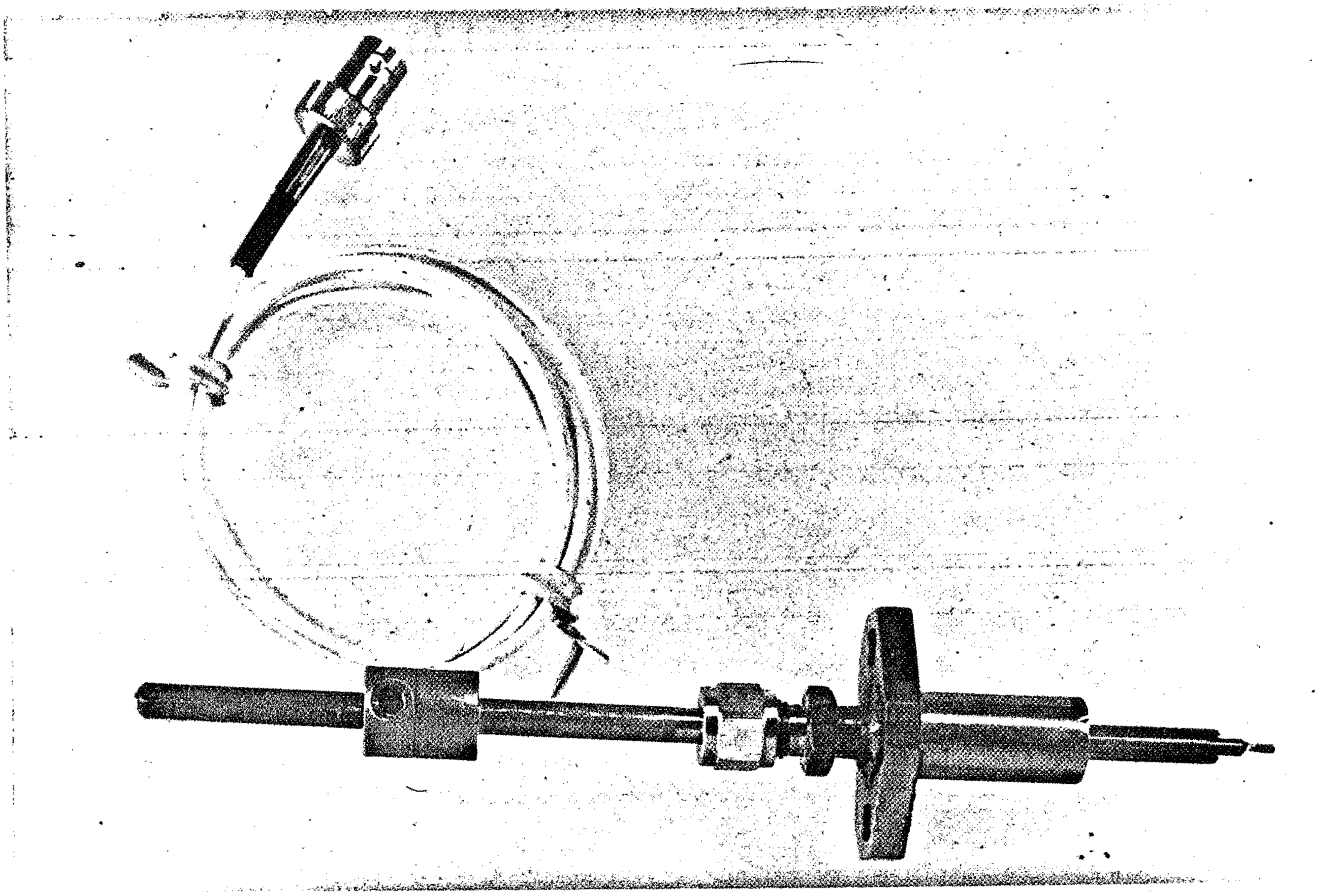

Figure 7 *Station 4 Probe Adaptor* *(77-441-9142)*

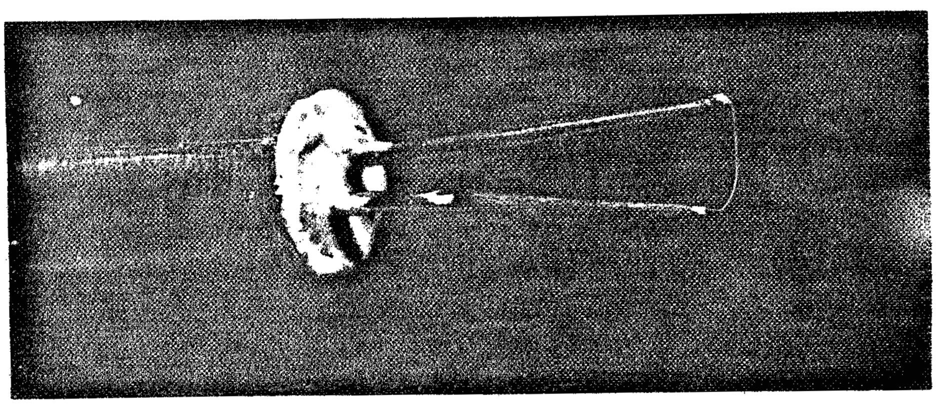

Figure 8 *Wire Probe* *(77-444-9002A)*

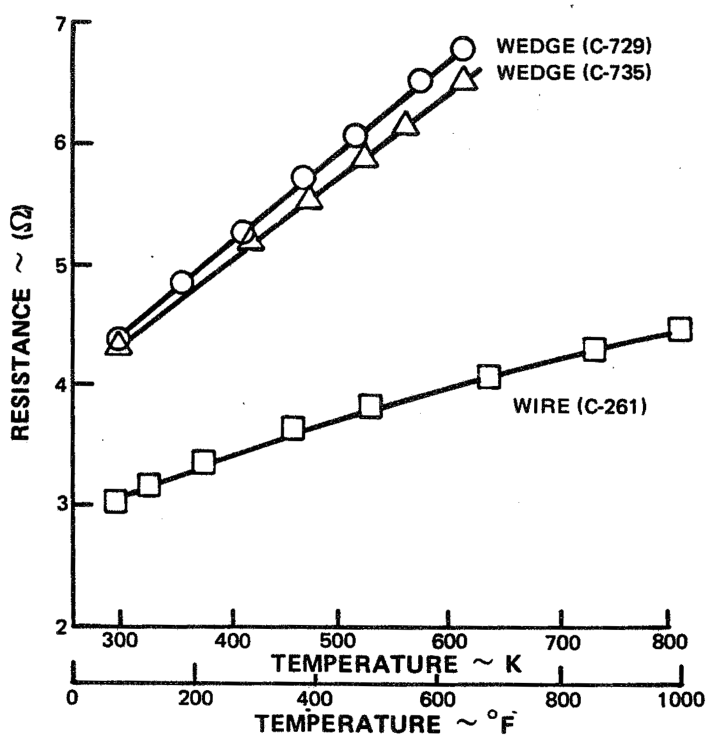

Figure 9 Dependence of Probe Resistance on Temperature

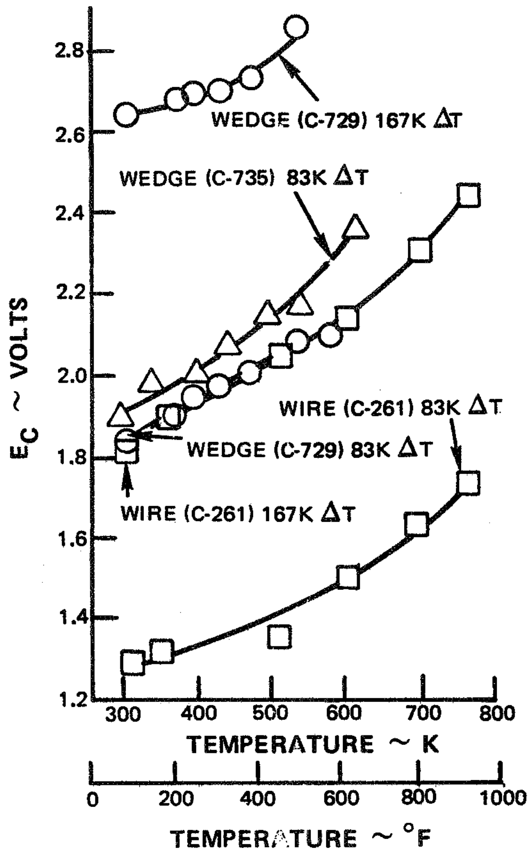

Figure 10 *Dependence of Quiescent Environment Bridge Voltage On Temperature*

31

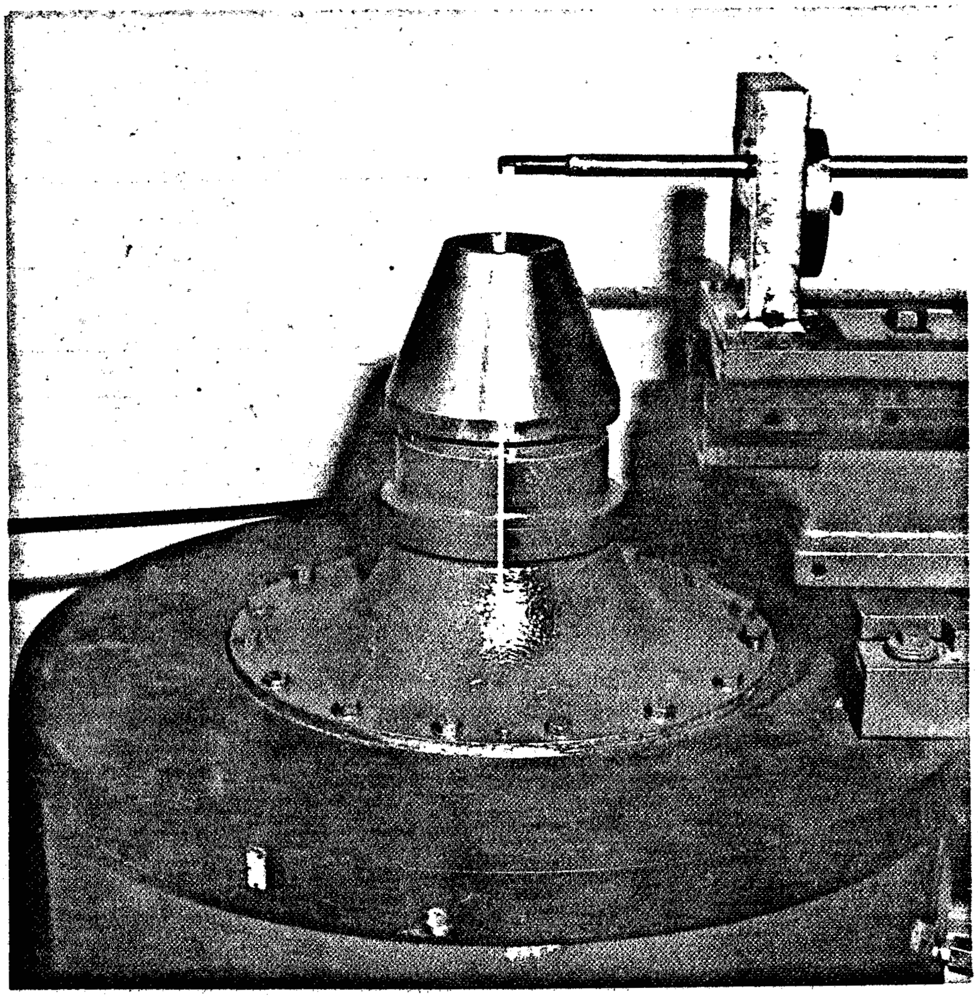

Figure 11 *Experimental Arrangement for Anemometer Velocity Calibrations* *(X-30941)*

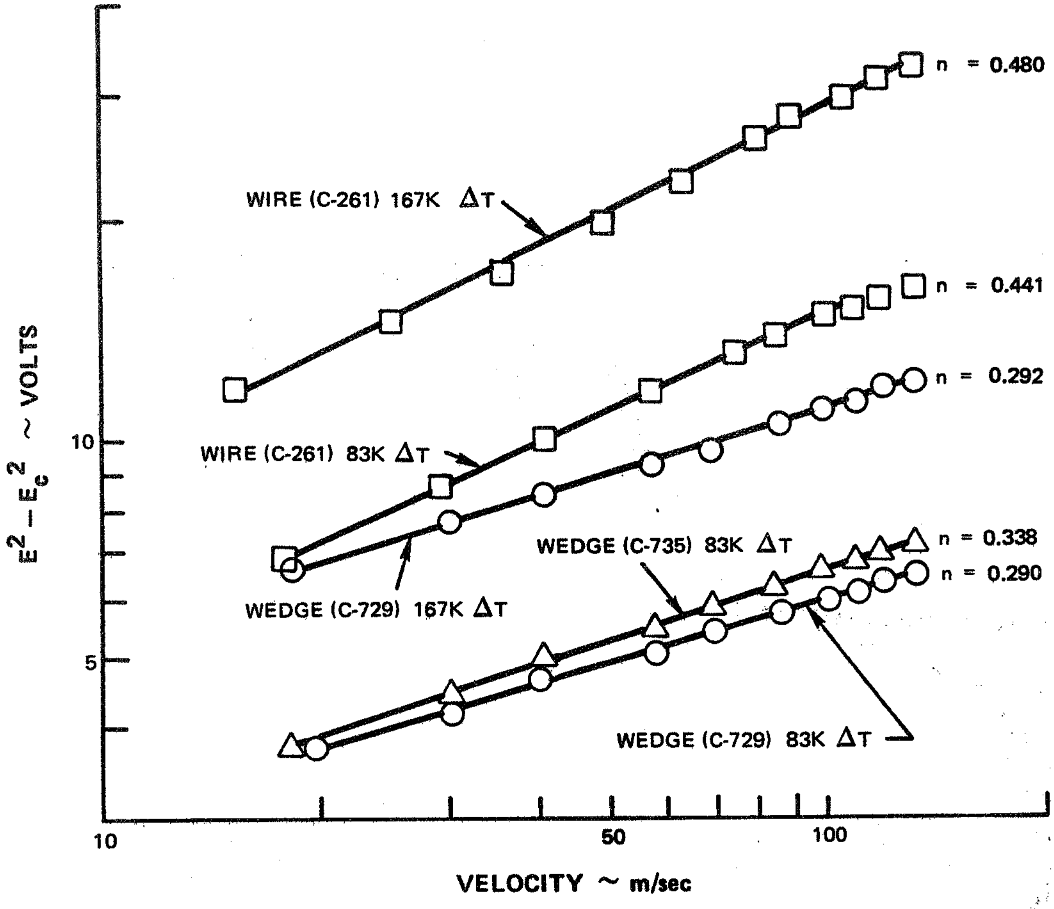

Figure 12 Anemometry Probe Velocity Calibrations

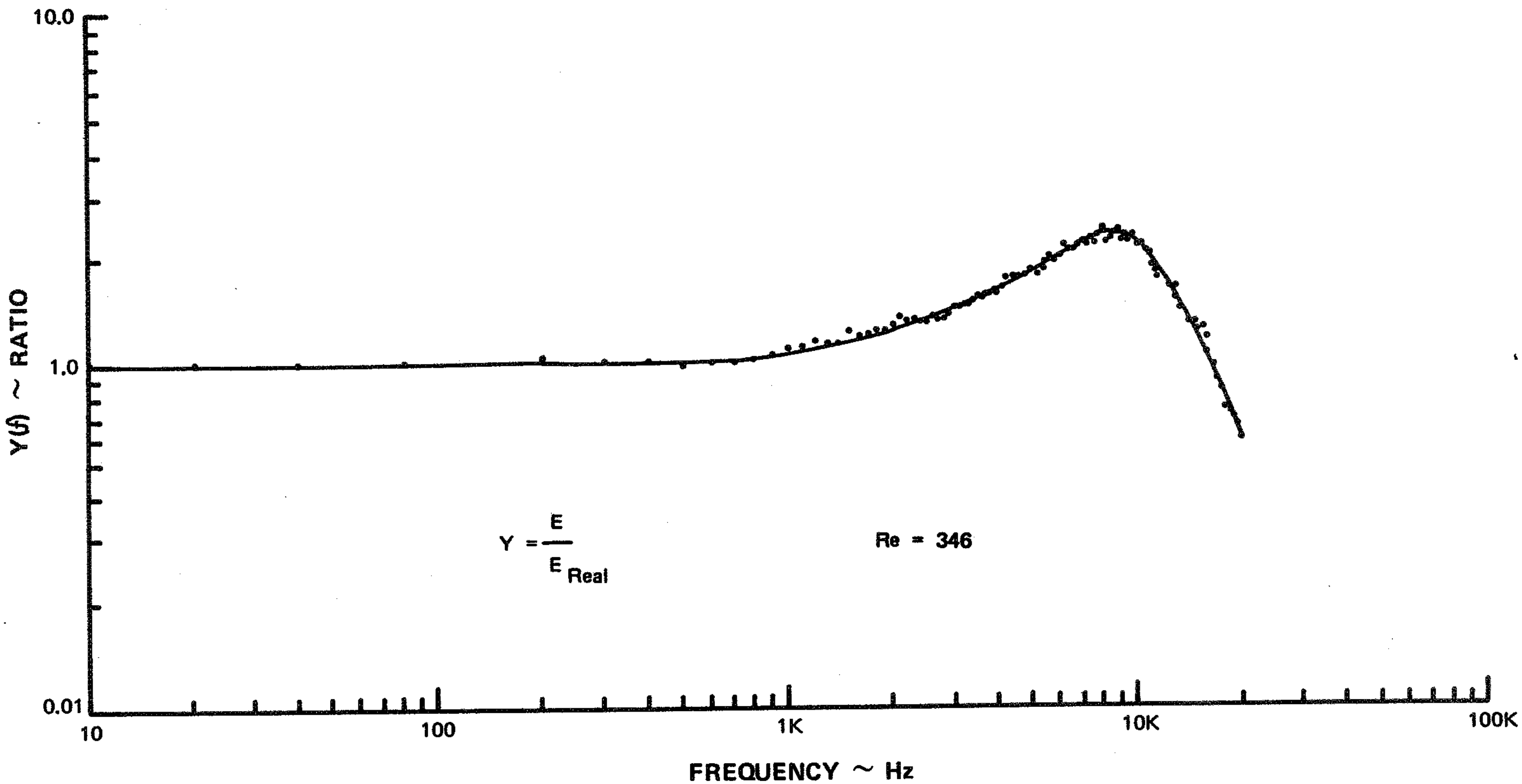

Figure 13 *Wedge Probe Transfer Function*

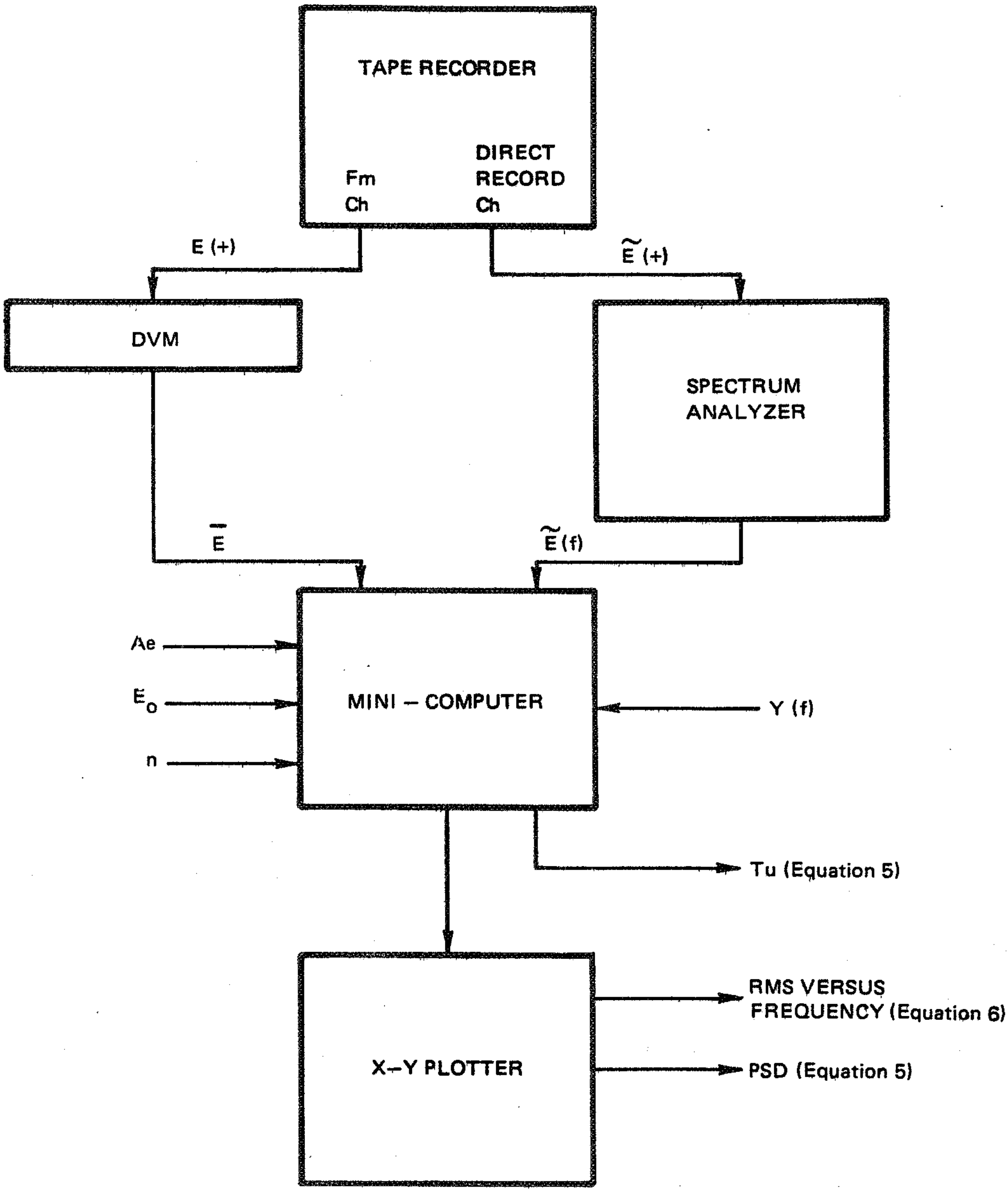

Figure 14 Block Diagram of Data Reduction System

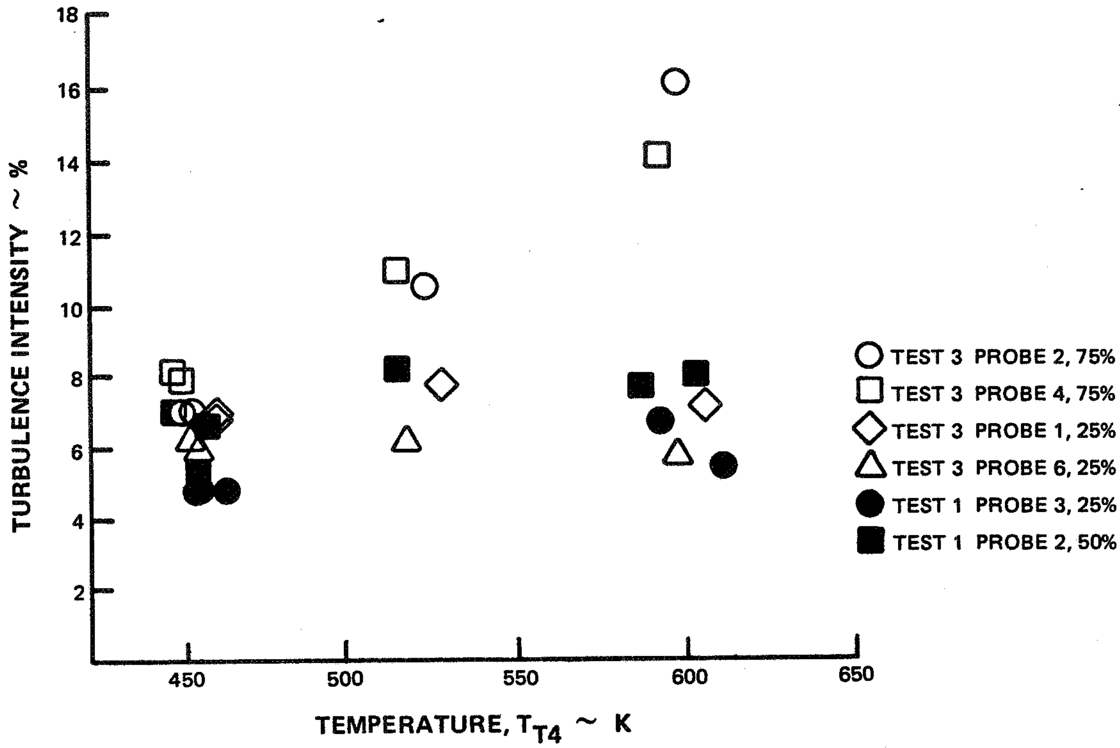

Figure 15 *Dependence of Turbulence on Engine Operation*

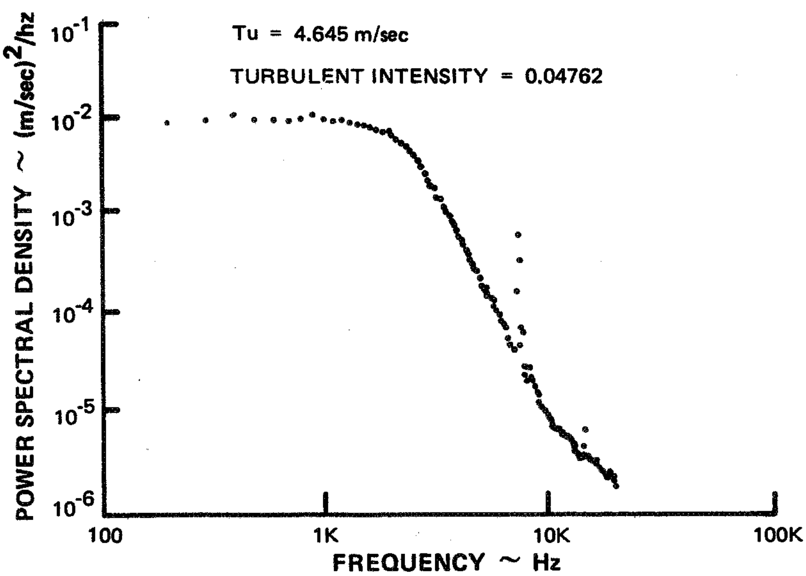

Figure 16 *Test 1, Probe 3 (Wedge Type) Power Spectral Density Function for Idle Condition at 25 Percent Span*

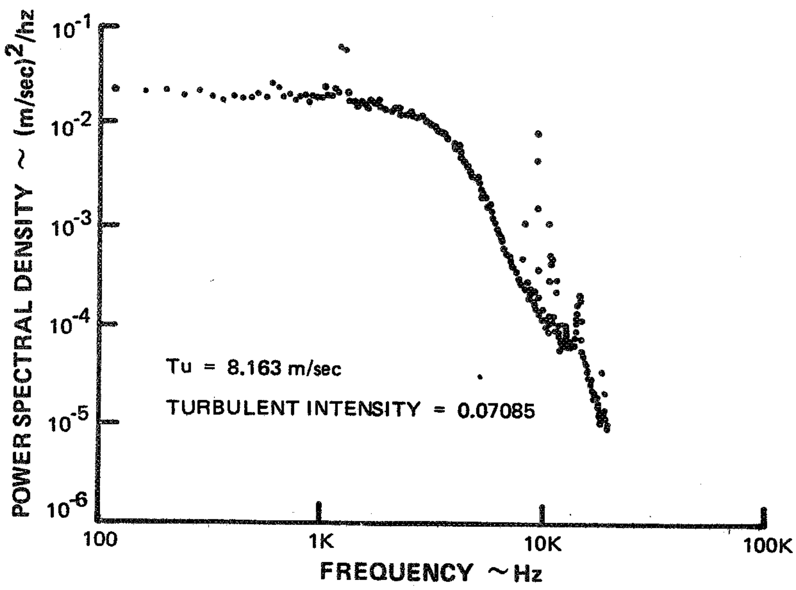

Figure 17 *Test 3, Probe 1 (Wedge Type) Power Spectral Density Function for Approach Power Condition at 25 Percent Span*

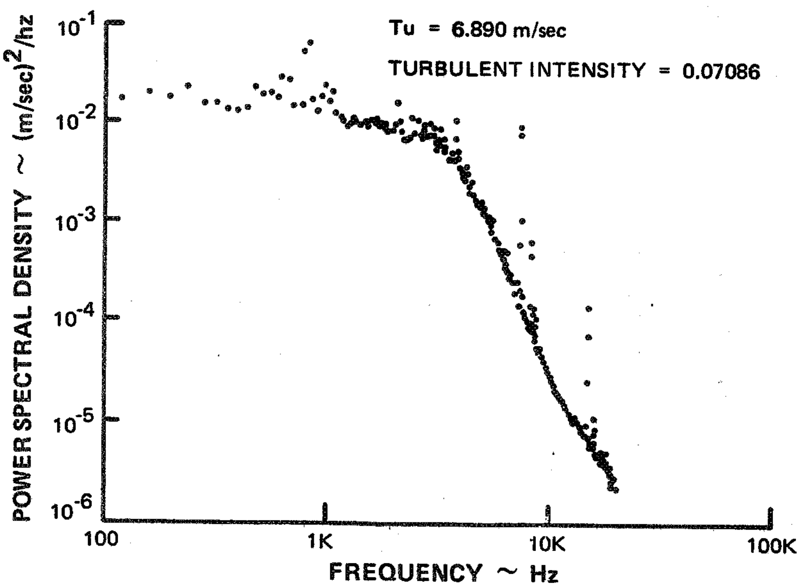

Figure 18 *Test 3, Probe 2 (Wedge Type) Power Spectral Density Function for Idle Condition at 75 Percent Span*

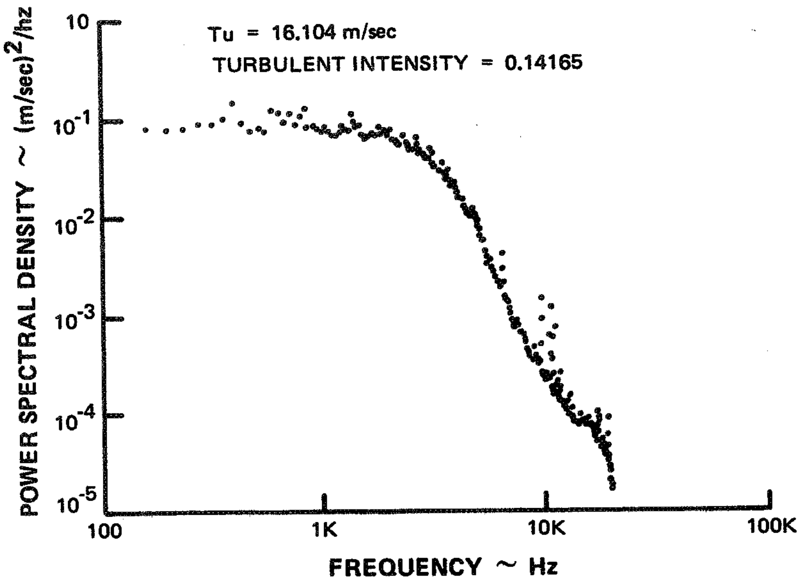

Figure 19 *Test 3, Probe 4 (Wedge Type) Power Spectral Density Function for Approach Power Condition at 75 Percent Span*

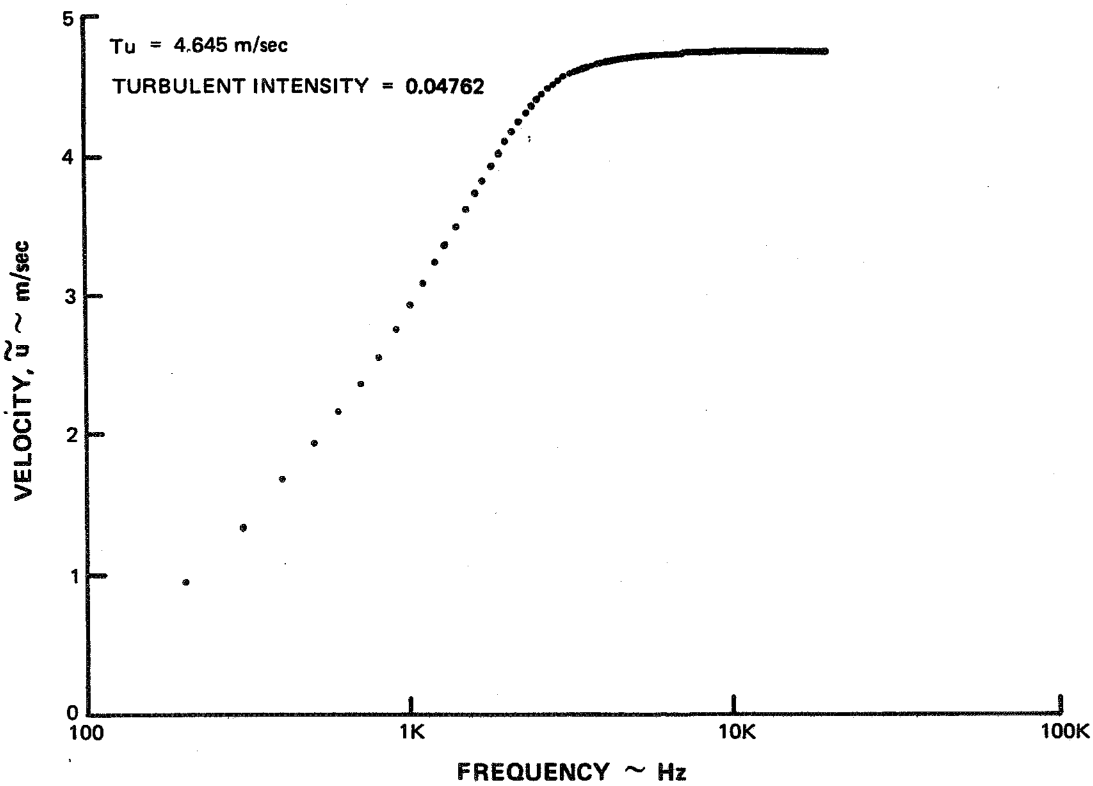

Figure 20 *Test 1, Probe 3 (Wedge Type) Spectral Distribution for Idle Condition at 25 Percent Span*

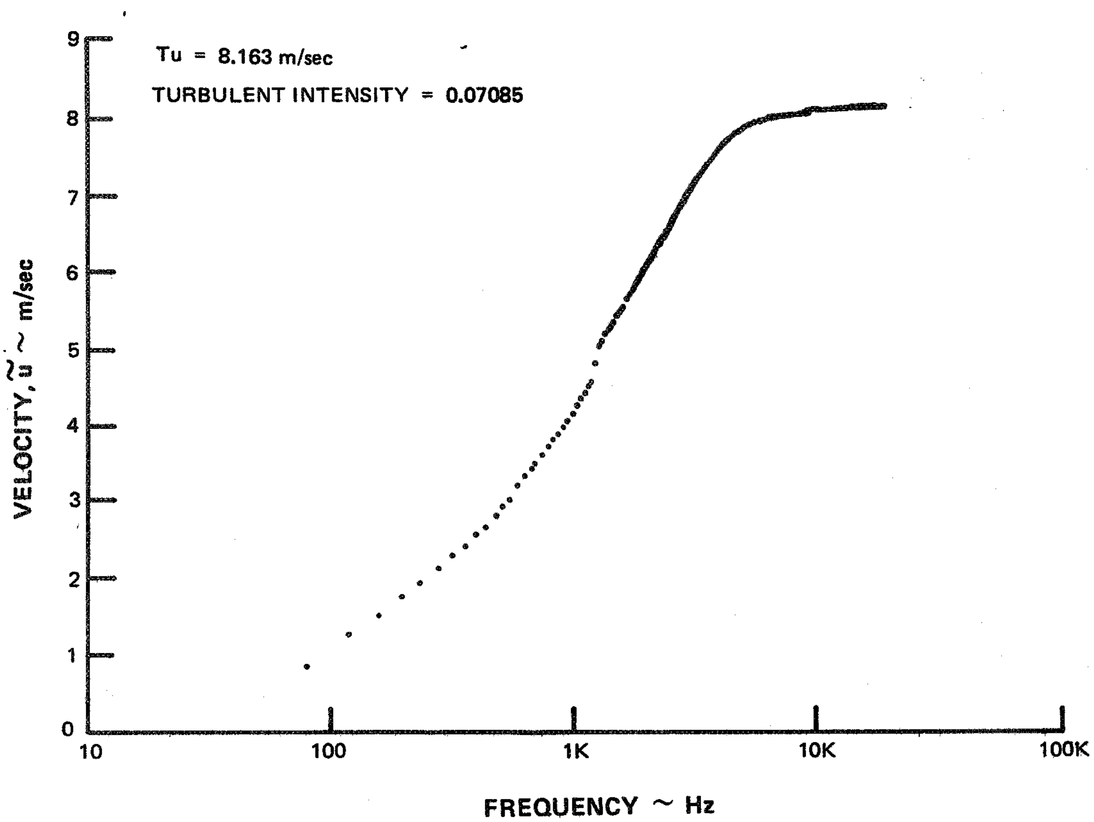

Figure 21 *Test 3, Probe 1 (Wedge Type) Spectral Distribution for Idle Condition at 25 Percent Span*

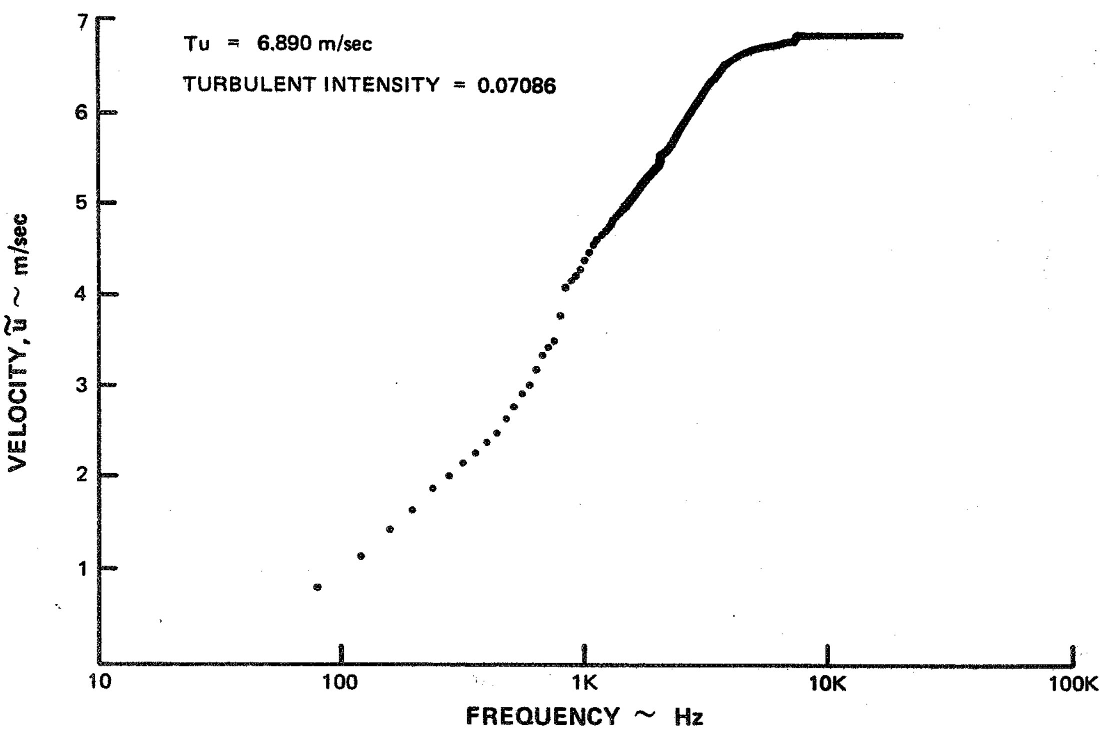

Figure 22 *Test 3, Probe 2 (Wedge Type) Spectral Distribution for Idle Condition at 75 Percent Span*

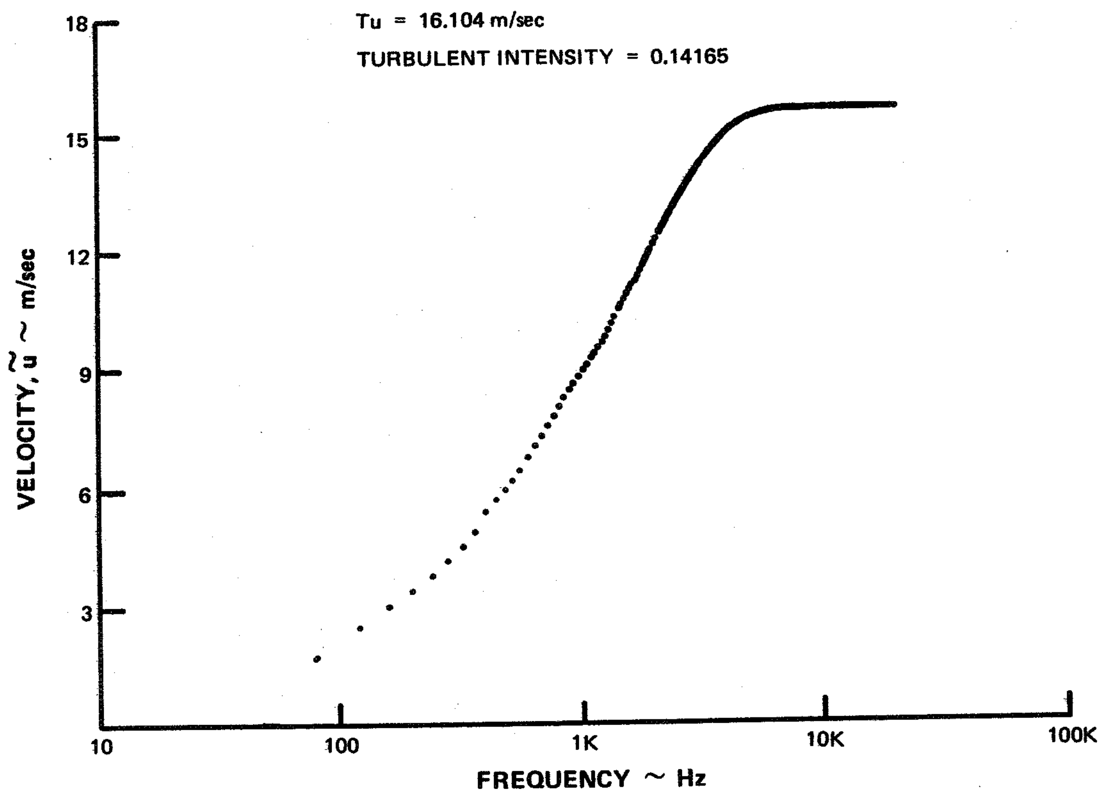

Figure 23 Test 3, Probe 4 (Wedge Type) Spectral Distribution for Approach Power Condition at 75 Percent Span

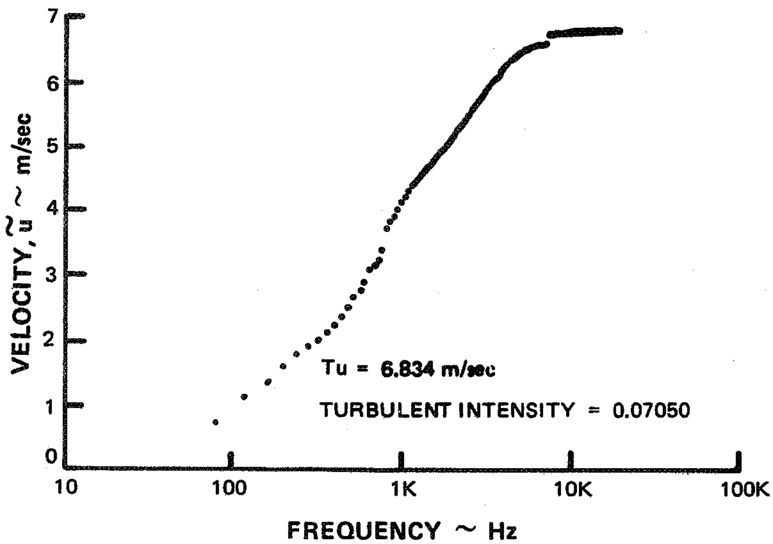

Figure 24 *Test 3, Probe 2 (Wedge Type) Spectral Distribution for Idle Condition at 75 Percent Span*

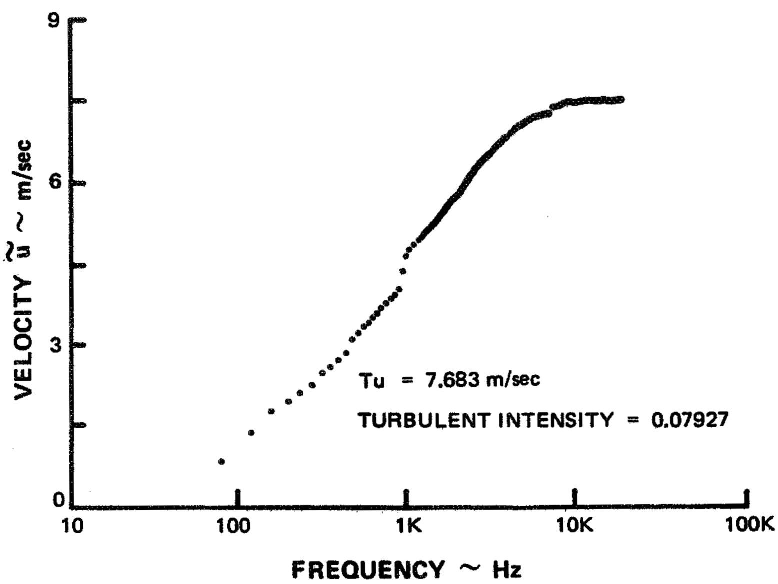

Figure 25 *Test 3, Probe 4 (Wedge Type) Spectral Distribution for Idle Condition at 75 Percent Span*

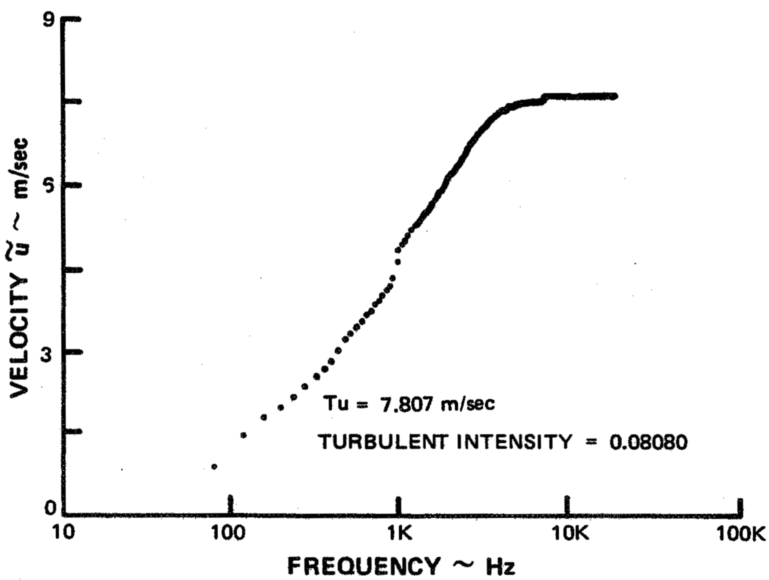

Figure 26 *Test 3, Probe 4 (Wedge Type) Spectral Distribution for Idle Condition at 75 Percent Span*